European Association for the Development of Renewable Energies, Environment and Power Quality

International Conference on Renewable Energies and Power Quality (ICREPQ'09)

Valencia (Spain), 15th to 17th April, 2009

Finite Element Analysis of Electrical Machines Used in Two-Frequency Indirect Temperature Rise Tests

E. Schlemmer

ELIN EBG Motoren GmbH
Elin-Motoren-Straße 1, 8160 Preding bei Weiz (Austria)
Phone number:+0043 3172 90606 2115, e-mail: **Erwin.Schlemmer@elinebgmotoren.at**

Abstract. Heat runs of large asynchronous machines (AM) are hardly ever conducted under load but with synthetic approaches, such as the two-frequency method. In its classical variant, the AM's stator is fed by two series-connected synchronous machines (SM) with different frequencies, for instance 50 and 40 Hz. While the 50 Hz voltage determines the AM's flux, the 40 Hz source causes an AM stator current close to its rated value. Together, voltage and current yield approximately full load losses in the AM without mechanical loading. For designing the amortisseurs of the synchronous generators, damper losses were calculated using the Finite Element method. Additionally, calculated full load AM losses were compared against their respective values for the two-frequency method.

Key words

Two-frequency method, temperature rise tests, asynchronous machine, synchronous machine, Finite Element method.

1. Introduction

Direct evaluation of induction motor efficiency using dynamometer tests or torque measurement, cf. [1], is hardly ever performed for machines of more than several 100 kW. The reasons for that are well known: (i) lack of a suitable load, (ii) impossibility of coupling vertical machines to a mechanical load in the test field, (iii) large efforts in terms of energy and time. Therefore, several methods for generating rated load losses without access to a mechanically coupled machine were devised. Besides the two-frequency (2f) method, described as early as 1921 by Ytterberg (according to [2]), several other approaches are known from the literature, for instance [3]. In the original 2f-method, the induction machine to be tested is fed by two synchronous generators with different frequency. Due to the fact that each synthetic load method runs the machine under very special conditions, an analytical treatment is usually rather cumbersome. For instance, Meyer ([2], [4], and [5]) states that the nonlinear system of equations describing an AM under 2f-conditions does not allow a closed analytical solution for variable speed of the induction machine and proceeds with an investigation of its stationary state and small deviations from that. The two voltage sources feeding the induction machine are considered as ideal, the linearized equations governing the excursions around the stationary state are solved iteratively. In a further step, Tietze ([6]) focuses on a system of three machines comprising the induction motor and two synchronous generators, both capable of speed oscillations. The underlying system of equations is solved numerically.
In this paper, the method of choice is the Finite Element (FE) method since it allows a detailed description of saturation and current displacement effects in the investigated machine. Moreover, rotor motion and external circuits can be incorporated quite effortlessly. However, the voltage sources have to be considered as ideal. The rationale behind the investigations described in this paper is the design of a test field capable of examining asynchronous machines with a rated power of more than 10 MW. This test field will be located in a factory for electrical machines presently being built near Weiz, Austria (Fig. 1).

Fig. 1. View of the new manufacturing plant for electrical machines, September 2008.

The two synchronous generators destined to act as sources in future two-frequency test runs were analysed with respect to the expected amortisseur currents and the torque pulsations imposing oscillating stress on their shafts.

2. Two-Frequency Method

The principle of the two-frequency method is depicted in Fig. 2. Two voltage supplies of different frequency are connected in series to drive an induction motor. The main source U_1 exhibits rated frequency f_1, the auxiliary source has a lower frequency f_2, about 60 to 95 % of f_1 and its magnitude ranges from 5 to 25 % of U_1. In practice, U_2 and f_2 are adjusted such that the induction motor is driven with rated rms values of both voltage and current. Without a coupled mechanical load, the induction machine oscillates between speeds determined by f_1 and f_2 thus acting alternately as motor and as generator. In order to reduce negative effects on the mains, two motor-generator sets are employed for the independent sources SM_1 and SM_2. For all simulations in this paper, f_1=50 Hz and f_2=40 Hz.

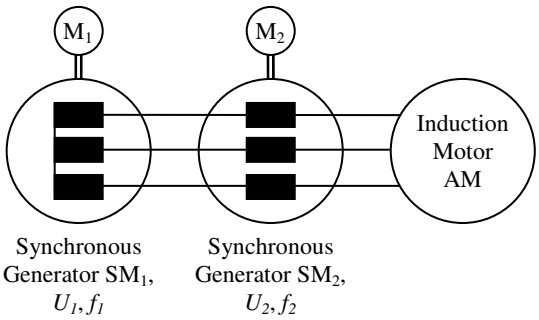

Fig. 2. Schematics of the two-frequency method comprising two synchronous generators.

3. Finite Element Simulations

A. Asynchronous Machine

In the case of the asynchronous machine (AM), the main emphasis lay on torque pulsations, the comparison of iron losses and the estimation of currents in the rotor cage. The cross section of the model under consideration can be seen in Fig. 3.

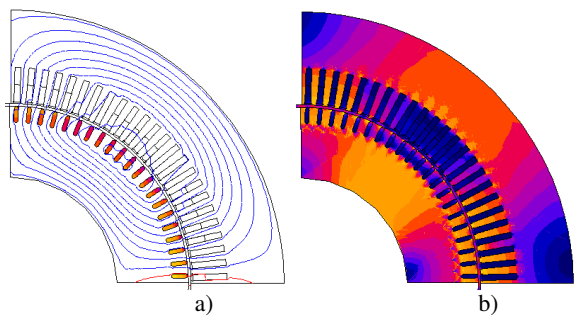

a) b)

Fig. 3. Induction motor, current density in the cage (a) and magnetic flux density (b).

The stator currents of AM are shown in Fig. 4 where the frequency sweep is easily discerned. Because of the two frequencies in the stator winding, the rotor cage carries substantial currents although no mechanical load is provided. Whereas the slip of the rotor with respect to the 50 Hz system in the stator is quite small, the slip regarding the 40 Hz system is about 20 per cent. Accordingly, 10 Hz currents are set up in the rotor cage with losses roughly equivalent to the respective load value in the cage.

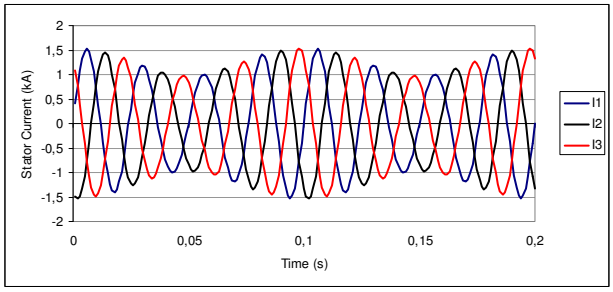

Fig. 4. Stator currents of AM and both SMs.

It can be inferred from the torque oscillations in Fig. 5 that the AM alternately works in motoring and in generating mode. Additionally to the speed variation due to the difference in frequency of 10 Hz, a decaying mechanical oscillation of roughly 1 Hz can be observed which is also present in the simulation of the load case. Because of the long computation time required for FE solutions, they were stopped before the mechanical oscillations completely died out.

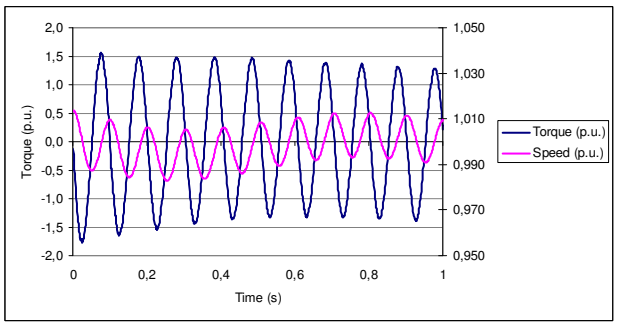

Fig. 5. Torque and speed oscillations of the asynchronous machine.

Fig. 6 shows the rotor copper losses during the initial stage of the two frequency computation. The mechanical oscillation of about 1 Hz can be observed in the losses as well. The copper losses amount to about 1,5 % of rated load which agrees well with the load test calculations and the estimations from the design program.

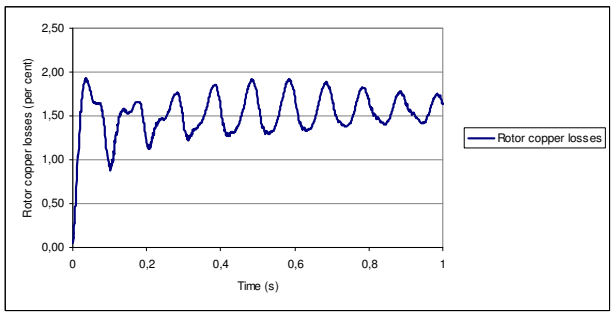

Fig. 6. Calculated rotor copper losses in per cent of rated load.

Although the agreement between direct load test and the bifrequency (2f) method was verified successfully on the experimental level ([2], [3]) and numerically ([7]), it was of some interest to compare iron and rotor copper losses of these two test methods by FE calculations. The

computed iron and rotor cage losses of the 2f method compared well against calculated iron losses of the load case as can be inferred from TABLE I.

TABLE I. – Calulated losses in p.u. of total losses

Case	Iron losses	Rotor copper losses
Load test	0,089	0,39
2f test	0,097	0,38

As in the literature, the calculated iron losses tend to be somewhat higher for the 2f case.

B. Synchronous Machines

SM_1 with rated frequency f_1 and voltage U_1 supplies the magnetisation current for AM. Additionally, it carries the much bigger load current of AM with frequency f_2 provided by SM_2. Consequently, due to the difference in rotation speed, SM_1 has to compensate the armature reaction of AM's load current in its damper winding. Fig. 7 illustrates the FE-model of SM_1 supplying f_1 while carrying massive damper currents due to the load current with f_2.

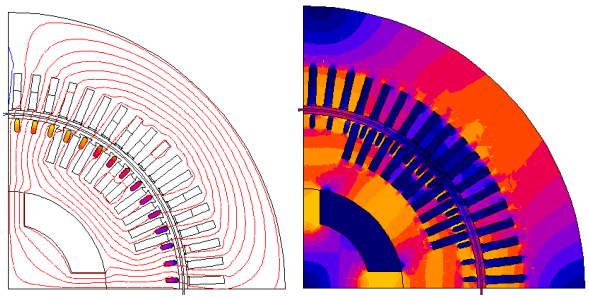

a) b)

Fig. 7. Synchronous machine SM_1, current density in the damper (a) and magnetic flux density (b).

Fig. 8 delineates torque and speed oscillations of SM_1 during the first few mechanical cycles of the two-frequency test.

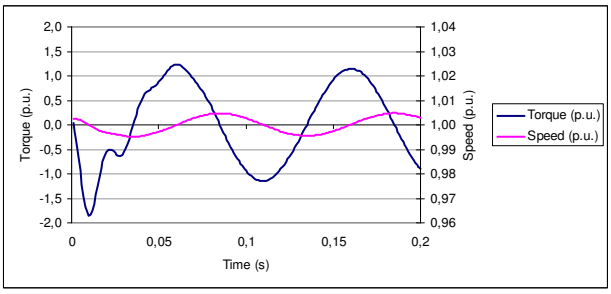

Fig. 8. Torque and speed oscillations of the synchronous machine SM_1.

Damper losses were calculated to about 0.5 % of rated power (Fig. 9), which required an enhanced damper concept. SM_1, running at 50 Hz, has to endure substantial 40 Hz currents in the stator which leads to considerable damper warming. SM_2, on the contrary, generates the 40 Hz system and sees light load only in terms of 50 Hz currents since these provide AM's magnetisation current. Consequently, the damper warming of SM_2 is negligible.

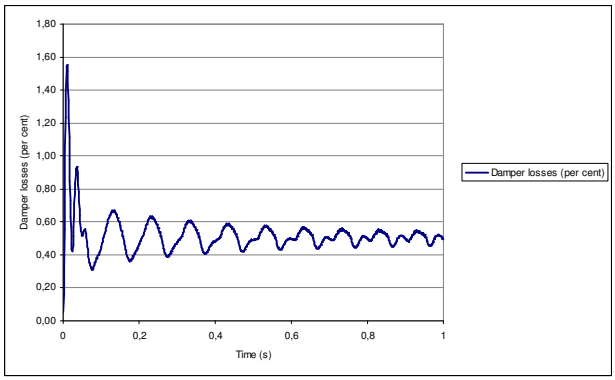

Fig. 9. Damper losses in SM_1 during the first second of the 2f run.

4. Simulation with a Lumped Parameter Model

A. Theoretical Background

The simulation of dynamic phenomena of synchronous machines can also be conducted by models based on Park's two-axis theory. The resulting system of differential equations is solved by a suitable time stepping method. For the description of the synchronous machine - based on Park's equations (1) to (6) and several minor extensions (7) to (9) - the following nomenclature is used.

u_{1d}, i_{1d} .....*d*-axis armature voltage and current

u_{1q}, i_{1q} .....*q*-axis armature voltage and current

u_2, i_2 .....field voltage and current

i_{3d}, i_{3q} .....damper currents in *d*- and *q*-axis

r_1, r_2 .....armature and field winding resistance

r_{3d}, r_{3q} .....damper resistance in *d*- and *q*-axis

l_{1d}, l_{1q} .....synchronous inductance in *d*- and *q*-axis

l_{hd}, l_{hq} .....armature reaction inductance in *d*- and *q*-axis

$l_{1\sigma}, l_{2\sigma}$ .....leakage ind. of armature and field winding

l_{23} .....mutual ind. between field and damper winding

$l_{3d\sigma}, l_{3q\sigma}$ ...damper winding leakage in *d*- and *q*-axis

m_T, T_J .....turbine torque, inertia constant

$\omega, \omega_s, \vartheta$ ...speed, synchronous speed, rotor angle

Since Park's formalism can be found in many textbooks on electric machinery, e.g. [8], [9], [10], the equations do not have to be discussed in more detail here. In order to take saturation into account, the armature reaction inductance is adjusted globally by the no-load saturation curve of the generator. The leakage inductances are also corrected for saturation since damper slot openings, for example, get heavily saturated under short circuit conditions. Accordingly, fault currents are substantially higher in the saturated case than with unsaturated leakage reactances.

$$u_{1d} = -r_1 i_{1d} - l_{1d}\frac{di_{1d}}{dt} - l_{hd}\frac{di_2}{dt} - l_{hd}\frac{di_{3d}}{dt} - \omega l_{hq} i_{3q} - \omega l_{1q} i_{1q} \quad (1)$$

$$u_{1q} = -r_1 i_{1q} - l_{1q}\frac{di_{1q}}{dt} - \omega l_{hd} i_2 + \omega l_{hd} i_{3d} - l_{hq}\frac{di_{3q}}{dt} + \omega l_{1d} i_{1d} \quad (2)$$

$$u_2 = r_2 i_2 + \left(l_{hd} + l_{23} + l_{2\sigma}\right)\frac{di_2}{dt} + \left(l_{hd} + l_{23}\right)\frac{di_{3d}}{dt} + l_{hd}\frac{di_{1d}}{dt} \quad (3)$$

$$0 = r_{3d} i_{3d} + \left(l_{hd} + l_{23}\right)\frac{di_2}{dt} + \left(l_{hd} + l_{23} + l_{3d\sigma}\right)\frac{di_{3d}}{dt} + l_{hd}\frac{di_{1d}}{dt} \quad (4)$$

$$0 = r_{3q} i_{3q} + \left(l_{hq} + l_{3q\sigma}\right)\frac{di_{3q}}{dt} + l_{hd}\frac{di_{1q}}{dt} \quad (5)$$

$$\frac{d\omega}{dt} = \frac{\omega_s^2}{2T_J}\left[i_{1d}\left(i_{1q} l_{1q} + i_{3q} l_{hq}\right) - i_{1q}\left(i_{1d} l_{1d} + i_{3d} l_{hd} + i_2 l_{hd}\right)\right] + \frac{\omega_s}{T_J} m_T\left(\vartheta\right) \quad (6)$$

$$\frac{d\vartheta}{dt} = \omega \quad (7)$$

$$l_{1d} = l_{hd} + l_{1\sigma} \quad (8)$$

$$l_{1q} = l_{hq} + l_{1\sigma} \quad (9)$$

B. *Speed Controller*

Equations (1) to (9) were implemented in a legacy design program for analysing generator transients. After several trial calculations, it became obvious that the generator speed during two frequency runs was subject to large variations. Since the 40 Hz-source was assumed to be ideal, the synchronous generator had a tendency to synchronize with the grid at 40 Hz. Therefore, it became necessary to enhance the program with a speed controller module as depicted in Fig. 10.

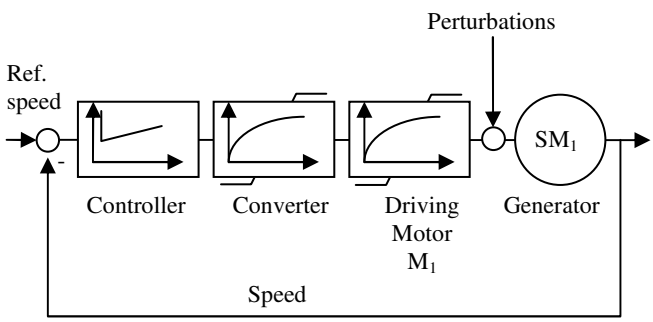

Fig. 10. Structure of the simplified drive train with speed controller.

The speed controller's action can be observed in Fig. 11. Without controller, the generator accelerates to slight overspeed and then decelerates in order to synchronize with the 40 Hz grid (not shown in the graph). With controller, after a short period of transients, the generator remains stable at 50 Hz. The ripple on the speed curves is due to the 10 Hz pulsations.

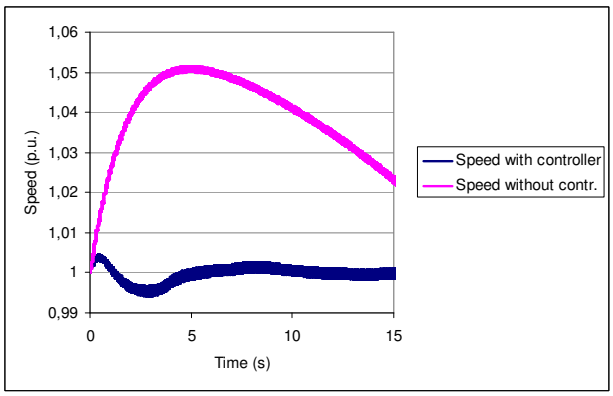

Fig. 11. Speed variations with and without speed controller.

The torque fluctuations during the initial stage are compared against the FE solutions in Fig. 12. Considering the coarse representation of saturation and damper circuits in the lumped parameter model, the agreement is very satisfactory.

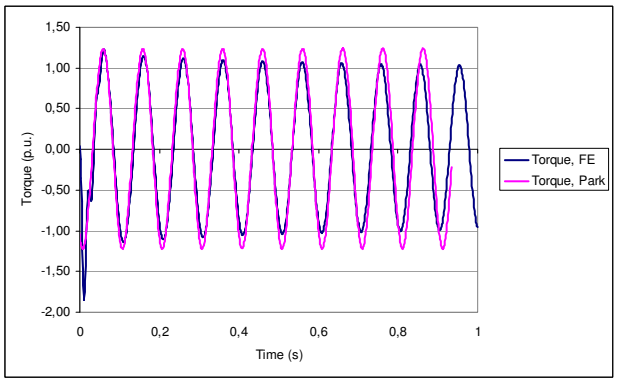

Fig. 12. Comparison of electromagnetic torque variations, FE-solution vs. model based on Park's equations.

Fig. 13 shows the speed fluctuations during a two frequency run after the speed has settled due to controller action. Most interestingly, even the low frequency oscillation due to the rotor's eigenfrequency is in the same order of magnitude as the FE solutions predicts.

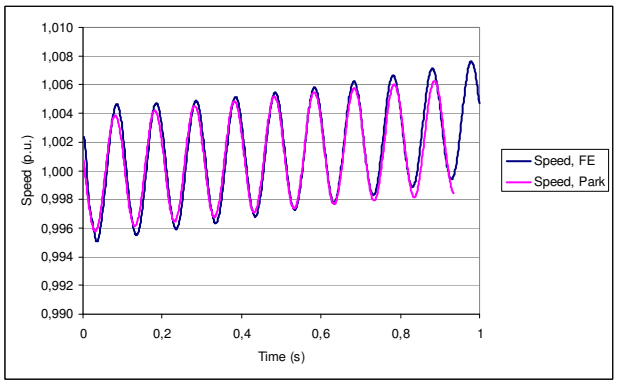

Fig. 13. Comparison of speed variations, FE-solution vs. model based on Park's equations.

C. *Torque Pulsations*

Since the electromagnetic torque oscillations occur at a frequency about ten times as high as the resulting eigenfrequency of the rotor, a variation of the generator's moment of inertia does not influence the magnitude of the torque pulsations significantly, as can be inferred from Fig. 14 and Fig. 15. For the actual value of the rotor's moment of inertia *J*, the speed excursions from the rated value are quite substantial. Needless to say that the assumption a much bigger machine (10**J*) would yield a signifcant reduction of the speed deviations, both with and without controller.

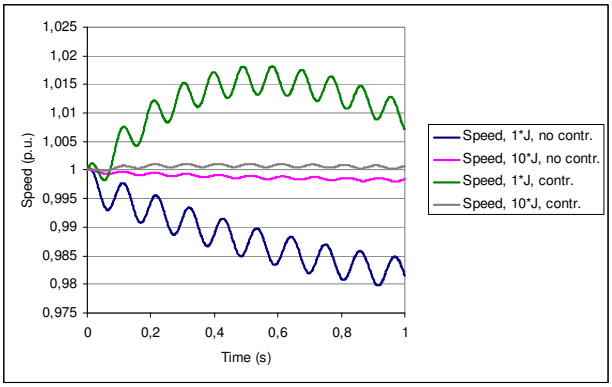

Fig. 14. Speed variation for d (1**J*: actual moment of inertia *J*, 10**J*: ten times this value), with and without speed control.

Since the torque variations are faster than the mechanical system can react in order to absorb or disperse kinetic energy, the magnitude of the electromagnetic torque pulsations is not noteworthily reduced (Fig. 15) by assuming a less rigid speed over torque characteristics. However, elastic effects of the drive train are not accounted for in this model. The torque variation in Fig. 15 is different from that of Fig. 12 because the total axis torque (including the torque applied by the drive) is displayed which settles to its stationary value after a few seconds after the decay of the transient phenomena.

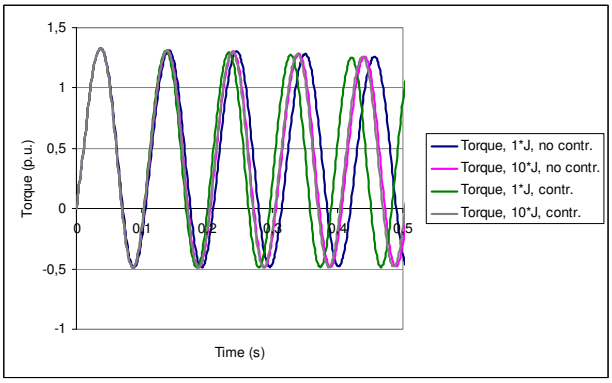

Fig. 15. Axis torque variation for the same parameter combinations as in Fig. 14.

5. Conclusion

The two-frequency method is an indirect temperature rise test. It allows a thermal loading of asynchronous machines similar to the conventional load test, albeit without mechanically coupled load. Besides questions concerning comparability of direct and indirect methods, design issues of the two synchronous machines serving as sources of different frequency had to be clarified. The Finite Element method (Flux2D) yielded answers in terms of losses, torque and speed oscillations as well as support for design decisions. Additionally, the FE solutions were compared against a model based on Park's equations which is considerably faster and yield sufficiently good results. With this model, the effects of speed control and the influence of the rotor's moment of inertia on the torque pulsations during a 2f-run could be investigated with negligible computational effort.

Acknowledgement

The author gratefully acknowledges the contribution of F. Müller, former head of the R&D department of VA TECH HYDRO GmbH, to the original version of the generator transients' analysis program.

References

[1] IEC 60034-2-1, Rotating electrical machines – Part 2-1: Standard methods for determining losses and efficiency from tests, *International Electrotechnical Commission*, Geneva, 2007.

[2] A. Meyer, „Das Betriebsverhalten von Asynchronmaschinen bei bifrequenter Speisung unter Berücksichtigung der Stromverdrängung im Rotor" (in German), *PhD-Thesis, ETH Zürich*, 1977.

[3] H. E. Jordan, J. H. Cook, and R. L. Smith, "Synthetic load testing of induction machines", *IEEE Trans. on Power Apparatus and Systems*, Vol. PAS-96, no. 4, pp. 1101-1104, July/August 1977.

[4] A. Meyer, "Erwärmungslauf von Asynchronmaschinen bei bifrequenter Speisung" (in German), *Bull. SEV/VSE* 68(1977)14, pp. 703-709, July 1977.

[5] A. Meyer and H. W. Lorenzen, "Two-frequency heat run – a method of examination for three-phase induction motors", *IEEE Trans. On Power Apparatus and Systems*, Vol. PAS-98, No. 6, pp. 2338-2347, Nov./Dec. 1979.

[6] T. Tietze, „Das Betriebsverhalten von Asynchronmaschinen bei bifrequenter Speisung unter Berücksichtigung drehschwingungsfähiger Synchrongeneratoren für Haupt- und Zusatznetz" (in German), *PhD-Thesis, TU München*, 1984.

[7] S. L. Ho and W. N. Fu, "Analysis of indirect temperature-rise tests of induction machines using time stepping Finite Element method", *IEEE Trans. on Energy Conversion*, Vol. 16, No. 1, pp 55-60, March 2001.

[8] K. Bonfert, *Betriebsverhalten der Synchronmaschine* (in German). Berlin: Springer-Verlag, 1962, p. 216.

[9] P. C. Krause, O. Wasynczuk, S. D. Sudhoff, *Analysis of electric machinery*. New York: IEEE Press, 1995, p. 220.

[10] G. Müller, *Theorie elektrischer Maschinen* (in German), Weinheim: VCH, 1995, p. 422.